

RADIATION EFFECTS ON STRAIN COMPENSATED QUANTUM DOT SOLAR CELLS

Cory D. Cress¹, Christopher G. Bailey¹, Seth M. Hubbard¹, David M. Wilt², Sheila G. Bailey², and Ryne P. Raffaelle^{2,*}

¹Rochester Institute of Technology, Rochester, NY 14623

²Photovoltaic and Space Environment Branch, NASA Glenn Research Center, Cleveland, OH 44135

E-mail: rprsp@rit.edu, Tel.: 585-475-5149

ABSTRACT

The effects of alpha-particle irradiation on the current-voltage characteristics and spectral responsivity of GaAs-based p-type / intrinsic / n-type solar cell devices containing 5-layers of InAs quantum dots (QD) grown with strain-compensation layers were investigated. The devices were subjected to ~4.2 MeV alpha-particle irradiation and the variation in the air mass zero short circuit current, open circuit voltage, fill factor, efficiency, and spectral responsivity were monitored as function of fluence and displacement damage dose. The measured spectral responsivity values of the quantum dot solar cell at wavelengths above and below the GaAs bandgap were used to investigate the rate of degradation in the InAs QDs in comparison to that of bulk GaAs. A computational model was developed to study the effects of strain on the energy threshold for atomic displacement (knock-out energy) of indium and arsenic within an InAs QD. Using the many-body Tersoff potentials, the energy of the primary knock-on atom occupying various sites within the lattice was calculated as a function of strain. The observed increases in minimum knock-out energy and interstitial-site energy with strain suggest a potential mechanism for the increased radiation tolerance observed in Stranski-Krastanow grown QDs.

INTRODUCTION

The dependence of space satellites on solar cell power systems has continually fueled the development of increased efficiency and radiation resistant devices. The incorporation of quantum dots (QDs) into traditional single or multi-junction crystalline solar cells is a potentially advantageous means for improving the overall conversion efficiency of photovoltaic devices. The tunable optical properties, isotropic absorption, and the potential for inter-sub-band absorption in QD arrays provide a potential for improving the matching between the spectral responsivity of such devices with that of the solar photon spectrum [1]. Devices containing QDs with appropriate band alignments have limiting efficiencies of ~50% when operating under the intermediate band effect and illuminated with 1000 suns [2]. A complimentary approach, one in which the QDs are used to shift the spectral bandwidth of the GaAs (or middle junction cell) of a conventional triple junction cell to longer wavelengths, has a one sun theoretical limiting efficiency of ~47% as derived by the detailed balance method [3].

Recently, the incorporation of Stranski-Krastanow grown InAs quantum dots (QDs) within the intrinsic region

of a GaAs p-type / intrinsic / n-type (*pin*) has been shown to have an improved end-of-life performance after exposure to alpha-particle irradiation over that of a reference GaAs *pin* device [4]. However, the beginning-of-life performance of this device suffered from considerable open circuit voltages losses, most likely resulting from strain-induced defects acting as deep level traps [4]. Furthermore, the presence of a modest threading dislocation density (e.g., $\sim 10^6 \text{ cm}^{-2}$) has been shown to reduce the introduction rate of deep level traps under 2 MeV proton irradiation in epitaxially grown GaAs layers [5]. The radiation tolerance observed in these devices, therefore, may be related to a similar effect.

To balance the strain present in QD laser diodes [6, 7] and multiple-quantum well solar cells [8], a layer of material under tensile strain is grown thereby offsetting the compressive strain leading to a strain-neutral stack. This technique has also been successful in InAs QD / GaAs *pin* devices whereby the open circuit voltage improved from 0.51 V to 0.85 V (baseline $V_{oc} = 1.01 \text{ V}$), and the short circuit current showed a slight improvement over the baseline [9, 10]. Therefore, the effects of alpha-particle irradiation on GaAs-based QD solar cells with higher beginning-of-life efficiencies and grown with strain compensation layers (GaP) will be investigated to determine whether the favorable radiation resistance observed in the non-strain compensated devices is related to the QDs or a result of the defects within the device.

There have been many reports in which an enhanced tolerance to ionizing radiation is demonstrated in QD arrays and QD lasers over similar bulk semiconductors or quantum well structures [11-15]. A commonality between these devices is the use of the strain-driven Stranski-Krastanow QD growth mode to achieve three-dimensional island formation. Regardless of whether the devices are grown with or without strain-compensation layers, strain fields are present within the QDs and surrounding barrier material. A better understanding of the improved radiation resistance in devices comprising QDs require the development of computational lattice bonding models which can be used to compare the structural properties of the QD constituents (e.g., In and As) in the relaxed and strained lattices. The Tersoff interatomic potentials are uniquely suited for this type of computational modeling as they employ analytically defined functions describing the 2-body (i.e., pair potentials) and 3-body interactions of an N-body system [16]. Models based solely on pair potentials (e.g., Lennard-Jones) favor the formation of close-packed structures, while the inclusion of the 3-body interactions provides a means to stabilize more open structures such as diamond and zinc blend [16]. The final

component of the Tersoff model is a bond-order dependent attraction term which varies the strength per bond depending on the local environment of the atom. This results in a more realistic attractive potential (especially in partially ionic systems) and allows for non-equilibrium bonding (e.g., bonds with atoms in interstitial sites) to be more accurately modeled [17]. To that end, a computational model based on the many-body Tersoff interatomic potentials was developed and used to calculate the threshold energy for lattice dislocation (E_{th}) of In and As atoms in relaxed and strained InAs. Increased E_{th} may have direct implications of increased radiation tolerance and longer device operational lifetimes, as fewer defects are generated per irradiating particle.

THEORETICAL

The threshold energy for atomic displacement E_{th} , dictates the level of non-ionizing damage that will be incurred by a semiconductor under irradiation. Just a small increase in E_{th} has a large effect on the total number of defects generated by a particle because the energy lost by the particle to the primary knock-on (PKO) atom and all subsequent collision events the PKO has with neighboring atoms requires more energy to create a defect. For instance, increasing the E_{th} of In and As atoms from 4.0 eV to 4.5 eV in a SRIM-2003 simulation of 5 MeV alpha-particles in InAs reduces the number of vacancies per alpha-particle from ~1800 to ~1650 [18, 19]. This corresponds to a reduction in vacancy generation by over 8%. The observed enhancement in radiation tolerance of the InAs QDs within the GaAs solar cells, therefore, suggests that there may be some physical property that is increasing the E_{th} within this material system. Besides the smaller size, the main property associated with these materials is the large compressive strain field which exists within the QDs [20-22]. With the use of the Tersoff interatomic potentials, the effect that a compressive strain field has on E_{th} is investigated. For a summary of the model and the parameters used see ref. [17, 23, 24].

This investigation is initiated by populating an InAs lattice with In and As atoms situated at their equilibrium positions, corresponding to a lattice parameter of 6.058 Å [17]. An In or As atom is chosen as the PKO situated at the (0,0,0) lattice position and the cohesive energy of the atom situated at this site is calculated by summing over the neighboring bonds as defined by the Tersoff potential model. A value of -3.107 eV is obtained which is consistent with the literature values [17, 23, 24]. The atom is then stepped throughout the lattice and at each point the cohesive energy of the atom is re-calculated. Initially, the goal is to determine the location of the interstitial sites, and the energy associated with those sites. An interstitial site may be defined as a local potential energy minimum, and can be found by plotting equi-potential surfaces with increasing energy. As depicted in Figure 1 the interstitial sites surround the basis atom situated at the ($a/4$, $a/4$, $a/4$) lattice position. In this figure the interstitial sites for an As atom in the InAs lattice are depicted. A similar result is

obtained for In although the energy of the sites are different. Differences arise because the In-In and As-As bonding have different energies associated with them.

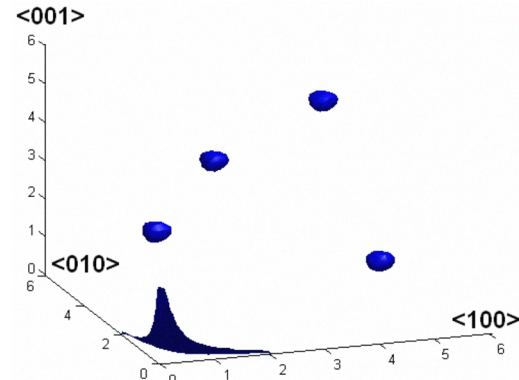


Figure 1. Equi-potential surfaces indicating the locations of local minima for As within the InAs lattice. Moving from left to right, the four blue spheres correspond approximately with the following crystal locations $(x,y,z) = (a/4, 3a/4, a/4)$, $(a/4, a/4, 3a/4)$, $(3a/4, 3a/4, 3a/4)$, and $(3a/4, a/4, a/4)$. The surface near $(0,0,0)$ corresponds to the top of the well (in energy) that the atom sits when in its equilibrium position. An In atom is located at $(a/4, a/4, a/4)$ and therefore these four interstitial sites surround that atom.

The threshold for displacement for a given direction, E_{th} is defined as the maximum energy encountered along a linear path before reaching a local minimum. For example, the black trace in Figure 2 depicts the potential energy of an In atom as it is displaced along the (201) direction towards an interstitial site near $(a, 0, a/2)$. Along this path, the atom approaches the face atom on the (100) plane, this causes the energy of the atom to peak at a displacement of ~4.2 Å before reaching the interstitial site. The difference between the peak energy and the energy of the atom at the equilibrium bonding site corresponds to the E_{th} for this particular direction.

Figure 2 also contains a trace depicting the effect of strain on the potential energy encountered by the atom along the same path. To simulate a strained InAs lattice, a compressive strain of ~7% in the x and y directions was assumed based on the difference in lattice parameters between InAs and GaAs. Additionally, the compressive strain in the x and y directions will cause the lattice to expand in the z-direction and for that a Poisson's ratio of 1/3 was assumed yielding a tensile strain of ~2.3 % in the z-direction. Strain has a profound effect on the E_{th} , along this direction; it is increased by over a factor of 2, and the energy of the interstitial site is also increased.

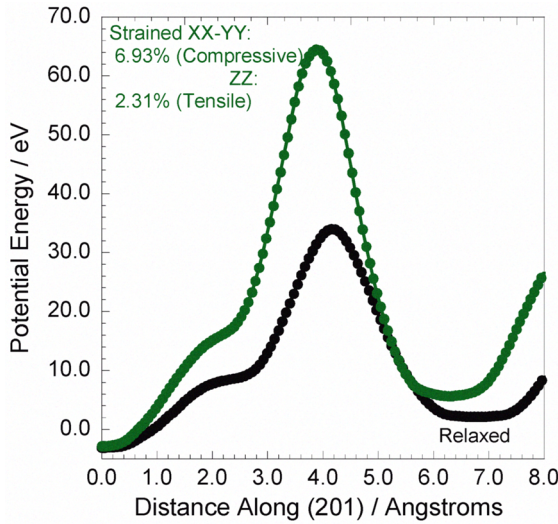


Figure 2. Potential energy of an Indium PKO along (201) for a relaxed InAs lattice (black trace) and a strained lattice (green trace).

The above example illustrates the large effect strain has on the threshold energy for displacement. However, the strain in quantum dots is not constant; theoretical calculations have predicted the strain to range from a maximum of ~7% compressive at the base of the quantum dot and slowly relax becoming slightly tensile at the peak (this was predicted for pyramidal InAs QDs on GaAs [20]). The effect of strain on the cohesive (potential) energy of the atom occupying its equilibrium site is depicted in Figure 3. As expected, the equilibrium energy increases with increasing strain indicating that the lattice is no longer arranged in the minimum energy configuration.

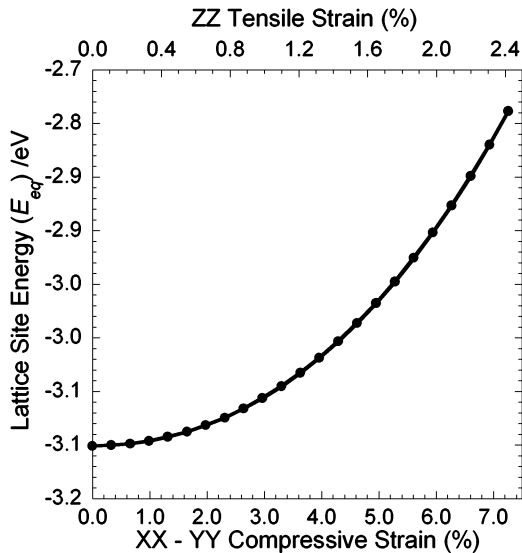


Figure 3. Effect of strain on the equilibrium lattice cohesive energy of the atom.

Furthermore, the effect of varying the strain on the knock-out energy lower bound for In and As PKOs reaching the specified interstitial site are depicted in Figure

4a and b, respectfully. In both cases increasing strain results in a slightly non-linear increase in the lower bound on the E_{th} which is defined as the difference between the interstitial site energy and the equilibrium bonding site energy ($E_i - E_{eq}$). This means the energy associated with the atoms occupying interstitial sites increases at a greater rate than that of the (0,0,0) site energy depicted above. This is considered the lower bound on the E_{th} because it is the minimum amount of energy required to force the PKO into the interstitial location while still conserving energy.

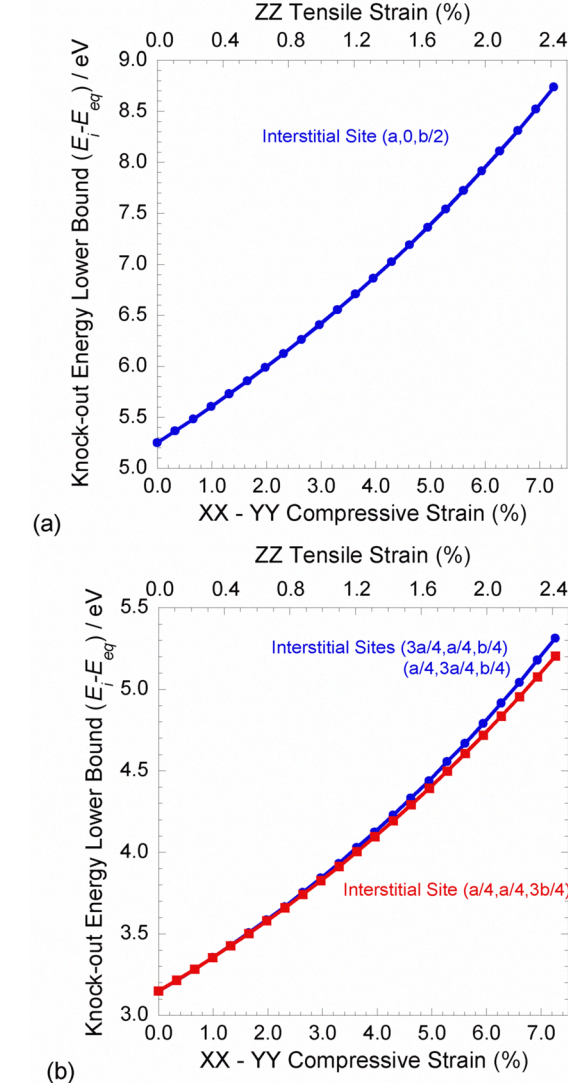


Figure 4. Effect of strain on the minimum knock-out energy required to reach the labeled interstitial sites for (a) In and (b) As as the PKO.

The above results have provided convincing arguments that strain has a large impact on the minimum energy to displace an atom. Furthermore, the increased potential energy associated with the interstitial energy sites suggests that dislocated atoms occupying these sites may be slightly more mobile. This fact, coupled with the non-uniform strain field present within the InAs QDs may

cause the atoms occupying interstitial sites and vacancies to migrate towards regions of tensile or compressive strain, respectively. The short distance required to reach the GaAs boundary in the QDs may act as a self healing effect within the quantum dots.

EXPERIMENTAL

The devices investigated in this study consist of a strain-compensated GaAs *pin* device and a reference GaAs device both 1 cm^2 in area with 4% grid shadowing. The strain compensated device (referred to as 5x QD) is comprised of 5-layers of InAs QDs, each separated by a 10 nm intrinsic GaAs cladding layer and a GaP strain relief layer, grown within the middle of the intrinsic region (14 Å). The device structure along with the OMVPE growth conditions have been reported elsewhere [10].

Irradiation of the devices was accomplished by placing the devices ~2 mm from a ^{210}Po alpha-particle source with an activity of 1 mCi and a circular area of 2.5 cm^2 . Upon reaching the device the alpha-particles have an average energy of 4.2 MeV which results in a range $\sim 12 \mu\text{m}$ [19]. The irradiation was performed in air under ambient conditions. The current density – voltage (*J-V*) characteristics and the spectral responsivity (*SR*) of the devices were measured after incremental increases in alpha-particle dose up to a total fluence of $4 \times 10^{12} \text{ alpha-particles/cm}^2$.

RESULTS AND DISCUSSION

The radiation response of the two devices was investigated by measuring the room temperature spectral responsivity and the current-voltage characteristics (AM0 illumination) as a function of alpha-particle irradiation. The variation in the *SR* of the two devices with irradiation in the region from 880 nm and below (not shown) is very similar; the greatest rate of degradation occurring in the longer-wavelength region of the spectra (830-880 nm). This suggests that the lifetime (and diffusion length) of holes in the base is reduced by the radiation induced defects making it less probable for them to diffuse to the junction when generated deep within the base.

The sub-gap region of the QDSC spectral responsivity for increasing levels of fluence are depicted in Figure 5a, along with the pre-irradiation and post $3.5 \times 10^{12} \text{ alpha-particles/cm}^2$ spectral responsivity curves for the baseline device. Pre-irradiation, the two devices demonstrate very similar spectral responsivity up to $\sim 880 \text{ nm}$ at which point the responsivity of the baseline device drops towards zero, while the responsivity of the QDSC is maintained as a result of the InAs QDs. For low-levels of fluence, the InAs QD responsivity peak shows little variation, but at very high fluences, it does decline significantly. Although the InAs QDs can be damaged by the alpha-particles, generation of defects within the GaAs barriers and the subsequent junction degradation will inherently contribute to the degradation observed in the measured spectral responsivity in this wavelength range. Even with these combined effects, the InAs QD degradation rate is much

lower than that of the bulk GaAs. This increased tolerance is likely a consequence of the increased energy threshold for atomic displacement in the strained InAs QDs as described above.

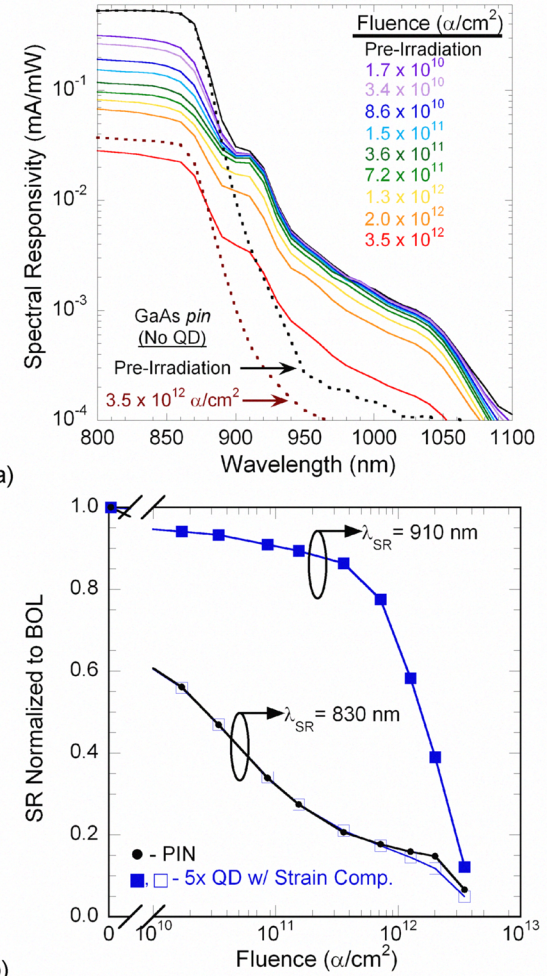


Figure 5. (a) Spectral responsivity of the QDSC at incremental levels of alpha-particle fluence; the pre-irradiation and post $3.5 \times 10^{12} \text{ alpha-particle}/\text{cm}^2$ responsivity spectra of the baseline device are overlaid for comparison. (b) The spectral responsivity as a function of fluence measured at 830 nm for both devices and at 910 nm for the QDSC.

The increased V_{oc} observed in the strain compensated QDSC, over that of the non-compensated QDSC device previously investigated [4], suggests that the concentration of defects within the junction has been significantly reduced by the strain compensation layers. It was originally suggested that the presence of such defects could reduce the rate of degradation in the device. Based on the current device performance, it appears that the defects were not the main contributor to the radiation tolerance observed in that device. Figure 5b contains the spectral responsivity as a function of fluence measured at 830 nm for both devices and at 910 nm for the 5x QD

device, which further illustrates the high tolerance observed in this figure that the InAs QD photogenerated current maintains >50% of its beginning-of-life value for two orders of magnitude more fluence than that of the bulk GaAs peak response.

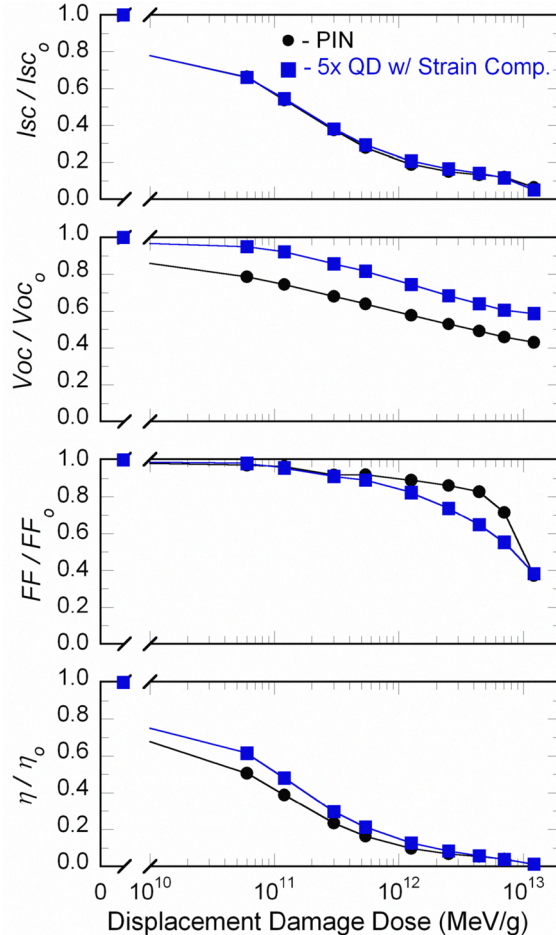


Figure 6. Normalized short circuit current, open circuit voltage, fill factor, and efficiency as a function of displacement damage dose for the baseline and the QDSC devices.

The variations in the normalized I_{sc} , V_{oc} , FF , and Efficiency with displacement damage dose are provided in Figure 6, for the baseline and the 5x QD devices. The displacement damage dose imparted to these cells by the isotropic alpha particle source was calculated using the method described in ref. [25], from which an effective non-ionizing energy loss ($NIEL_{eff}$) of 3.51 MeVcm²/g was obtained. The displacement damage dose for each point is the product of this and the total fluence imparted to the device. The 5x QD device maintains a much greater normalized V_{oc} as compared to the baseline devices which suggests that the QDs are improving the tolerance of the overall device not just in the sub-gap spectral responsivity. This improved V_{oc} leads to a greater normalized efficiency than that of the baseline device until a displacement

damage dose of $\sim 2 \times 10^{12}$ MeV/g, at which point both devices have degraded to less than 5% of their beginning-of-life efficiency. It should be noted that the actual V_{oc} of the QDSC (0.81 V after cleaving) was lower than that of the baseline device (0.95 V after cleaving) but the slower rate of degradation caused it to exceed the baseline device after reaching a displacement damage dose of $\sim 2 \times 10^{12}$ MeV/g.

CONCLUSIONS

In conclusion, a computation lattice binding modeling has been developed and illustrates that a physical property of Stranski-Krastanow grown InAs QD, namely strain, can lead to an increased threshold for lattice defect generation. This may lead to an increased radiation tolerance and may, in part, explain the increased radiation resilience observed in the experimental results of the InAs QD /GaAs pin solar cells exposed to alpha-particle irradiation. Improved defect mobility combined with the small size of the QDs leading to a self healing mechanism whereby defects diffuse to the InAs / GaAs interface has been suggested as a second mechanism for increasing the radiation tolerance of the materials. The radiation dependence of strain compensated InAs QD / GaAs solar cells have been invested in reference to a baseline GaAs device. Increased resilience in the V_{oc} and in the sub-GaAs responsivity of the QDSC was observed in the experimental results of the InAs QD /GaAs solar cell exposed to alpha-particle irradiation.

ACKNOWLEDGEMENTS

The authors would like to thank Dr. John Andersen for insightful discussions regarding the Tersoff potential energy model and Stephen J. Polly for his assistance in preparing the manuscript and presentation.

This work was supported by the DOD and the AFOSR under the contract No. FA95500610319. Additionally, C.D.C would like to acknowledge funding by NASA under a GSRP fellowship award No. NNX07AR57H

REFERENCES

- [1] D. Bimberg, M. Grundmann, and N. N. Ledencov, *Quantum Dot Heterostructures*: John Wiley and Sons, 1999, pp. 338.
- [2] A. Marti, L. Cuadra, and A. Luque, *Physica E*, **14**, 2002, pp. 150-157.
- [3] R. P. Raffaele, S. Sinharoy, J. Andersen, D. M. Wilt, and S. G. Bailey, "Multi-Junction Solar Cell Spectral Tuning with Quantum Dots," *Proceedings of World Conference on Photovoltaic Energy Conversion*, 2006, 162-166.
- [4] C. D. Cress, S. M. Hubbard, B. J. Landi, R. P. Raffaele, and D. M. Wilt, *Applied Physics Letters*, **91(18)**, 2007, pp. 183108.

- [5] M. González, C. L. Andre, R. J. Walters, S. R. Messenger, J. H. Warner, J. R. Lorentzen, A. J. Pitera, E. A. Fitzgerald, and S. A. Ringel, *J. Appl. Phys.*, **100**, 2006, pp. 034503/1-034503/7.
- [6] P. Lever, H. H. Tan, and C. Jagadish, *Appl. Phys. Lett.*, **95**, 2004, pp. 5710.
- [7] N. Nuntawong, S. Birudavolu, C. P. Hains, S. Huang, H. Xu, and D. L. Huffaker, *Appl. Phys. Lett.*, **85(3050)**, 2004.
- [8] M. Mazzer, K. W. J. Barnham, I. M. Ballard, A. Bessiere, A. Ioannides, D. C. Johnson, M. C. Lynch, T. N. D. Tibbits, J. S. Roberts, G. Hill, and C. Calder, *Thin Film Solids*, **76**, 2006, pp. 511-512.
- [9] S. M. Hubbard, C. D. Cress, C. G. Bailey, D. M. Wilt, S. G. Bailey, and R. P. Raffaelle, *Appl. Phys. Lett.*, **92(12)**, 2008, pp. 123512 /1-3.
- [10] S. M. Hubbard, R. P. Raffaelle, R. Robinson, C. Bailey, D. M. Wilt, D. Wolford, W. Maurer, and S. Bailey, "Growth and Characterization of InAs Quantum Dot Enhanced Photovoltaic Devices," *Proceedings of Proceedings of the Materials Research Society*, 2007, 1017E.
- [11] F. Guffarth, R. Heitz, M. Geller, C. Kapteyn, H. Born, R. Sellin, A. Hoffmann, D. Bimberg, N. A. Sobolev, and M. C. Carmo, *Appl. Phys. Lett.*, **82(12)**, 2003, pp. 3.
- [12] R. Leon, S. Marcinkevicius, J. Siegert, B. Cechavicius, B. Magness, W. Taylor, and C. Lobo, *IEEE Trans. Nucl. Sci.*, **49(6)**, 2002, pp. 2002.
- [13] R. Leon, G. M. Swift, B. Magness, W. A. Taylor, Y. S. Tang, K. L. Wang, P. Dowd, and Y. H. Zhang, *Appl. Phys. Lett.*, **76(15)**, 2000, pp. 3.
- [14] P. G. Piva, R. D. Goldberg, I. V. Mitchell, D. Labrie, R. Leon, S. Charbonneau, Z. R. Wasilewski, and S. Fafard, *Appl. Phys. Lett.*, **77(5)**, 2000, pp. 3.
- [15] W. V. Schoenfeld, C.-H. Chen, P. M. Petroff, and E. L. Hu, *Appl. Phys. Lett.*, **73(20)**, 1998, pp. 3.
- [16] J. Tersoff, *Phys. Rev. B.*, **39 (8)**, 1989.
- [17] P. A. Ashu, J.H.Jefferson, A.G.Cullis, W. E. Hagston, and C. R. Whitehouse, *J. Crystal Growth*, **150**, 1995, pp. 176-179.
- [18] J. F. Ziegler, *J. Appl. Phys. / Rev. Appl. Phys.*, **85**, 1999, pp. 1249-1272.
- [19] J. F. Ziegler, J. P. Biersack, and U. Littmark, *The Stopping and Range of Ions in Solids*, vol. 1. New York: Pergamon Press, 1985.
- [20] D. Bimberg, M. Grundmann, and N. N. Lednetsov, *Quantum Dot Heterostructures*, vol. 1. Chichester: John Wiley and Sons, 1999.
- [21] S. M. Hubbard, R. P. Raffaelle, R. Robinson, C. Bailey, D. M. Wilt, D. Wolford, W. Maurer, and S. Bailey, "Growth and Characterization of InAs Quantum Dot Enhanced Photovoltaic Devices," *Proceedings of Proc. of the Materials Research Society Spring Meeting*, 2007.
- [22] S. M. Hubbard, D. M. Wilt, S. Bailey, D. Byrnes, and R. P. Raffaelle, "OMVPE Grown InAs Quantum Dots for Application in Nanostructured Photovoltaics," *Proceedings of Proc. of the World Conference on Photovoltaic Energy Conversion*, 2006, 118-121.
- [23] K. Albe, K. Nordlund, J. Nord, and A. Kuronen, *Physical Review B*, **66(3)**, 2002, pp. 035205.
- [24] M. A. Migliorato, A. G. Cullis, M. Fearn, and J. H. Jefferson, *Phys. Rev. B.*, **65**, 2002, pp. 115316.
- [25] C. D. Cress, B. J. Landi, and R. P. Raffaelle, *IEEE Trans. Nucl. Sci.*, **55(3)**, 2008.